

Stepwise Reduction of β -Trioxopyrrocorphins: Collapse of the Oxo-induced Macrocycle Aromaticity

Nivedita Chaudhri,^{*a} Matthew J. Guberman-Pfeffer,^{a,†} Matthias Zeller,^b and Christian Brückner^{*a}

^a Department of Chemistry, University of Connecticut, Storrs, CT 06269, USA.

^b Department of Chemistry, Purdue University, West Lafayette, IN 47907, USA

ABSTRACT: The diatropic ring current that characterizes the unexpectedly aromatic octaethyltrioxopyrrocorphins gets drastically reduced upon chemical reduction of one and particularly two ketone moieties. With increasing reduction, the chromophores containing one pyrrole, one/two pyrrolinone, and one/two pyrrolines, respectively, become more similar to regular, non-macrocyclic-aromatic pyrrocorphins (hexahydroporphyrins). Single crystal diffraction shows the reduction products to be idealized planar. With increasing reduction, their UV-vis spectroscopic signatures are those of conjugated but non-aromatic oligopyrroles. Their diatropic ring current, as assessed by ¹H NMR spectroscopy, showed them to possess largely non-aromatic π -systems. Dihydroxylation of select β,β' -dioxo-bacteriochlorin and β,β' -dioxoisobacteriochlorins also resulted in the formation of equivalent mixed pyrrole/two pyrrolinone/pyrroline chromophores. Computations were able to reproduce the experimental trends of the diatropic ring currents and filled in the data for the regioisomers that could not be experimentally accessed. The work further highlights the electronic influence of the β -oxo-substituents and, more specifically, the origin of the aromaticity of the trioxopyrrocorphins. It also presents a series of chemically robust pyrrocorphins, a chromophore class for which many chemically very sensitive members have been reported.

INTRODUCTION

The sequential reduction of one, or both, cross-conjugated β,β' -double bonds of the porphyrins generates chlorins, bacteriochlorins or isobacteriochlorins, respectively (Figure 1).¹

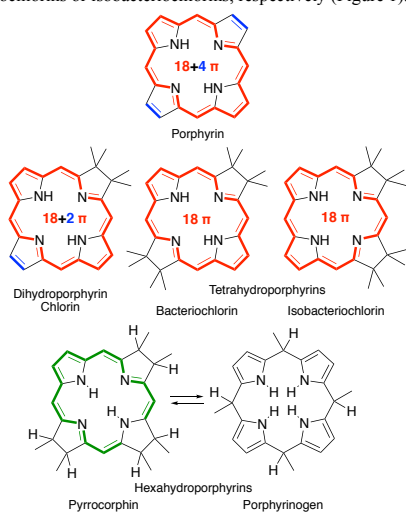


Figure 1. Framework structures of the hydroporphyrin classes indicated. The conjugation pathway of the central aromatic 18 π -electron system generally recognized to be present in (hydro)porphyrinoids is highlighted in red,^{1b} cross-conjugated, pseudo-olefinic

double bonds in blue. Conjugated, but non-aromatic, system in green.

The 18+4, 18+2, or 18 π -electron Hückel-aromatic systems of the (hydro)porphyrins are primarily responsible for their characteristic optical spectra (i.e., electronic properties, in general).² Removal of an additional double bond from the tetrahydroporphyrins results in the interruption of the Hückel-aromatic 18 π electron system and the formation of a non-aromatic pyrrocorphin or its *leuco*-form tautomer, a porphyrinogen.³

Eschenmoser and co-workers pioneered the studies of synthetic β -alkylpyrrocorphins, such as compound **1Mg**, in the context of their vitamin B₁₂ total synthesis (Figure 2).^{3a,4} Later studies on synthetic pyrrocorphins expanded the understanding of these hexahydroporphyrins.^{3b,5} Examples of pyrrocorphins derived from *meso*-pentafluorophenylporphyrin emerged more recently.^{3b,6} For instance, triple-cycloaddition formed pyrrocorphins **2/2NI^{6b}** and reduction of a bacteriochlorin-type bis-adduct realized pyrrocorphin **3^{6d}**; these pyrrocorphins formed fortuitously next to the target compounds. Unlike the traditional hexahydroporphyrins that were considered to be chemically sensitive molecules, particularly with respect to oxidation by air, no particular instability was noted for **2** and **3**. β -Oxo-functionalization seems to be an additional stabilization factor, as seen in porholactone-based pyrrocorphin analogue **4**.^{6c}

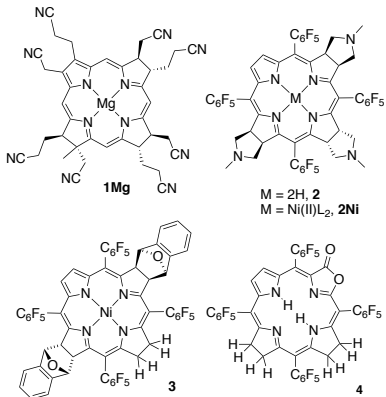
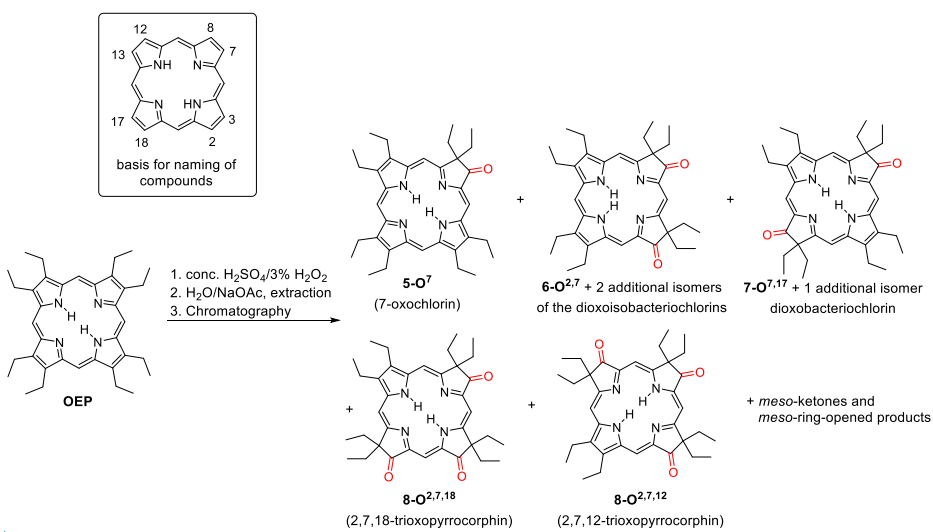


Figure 2. Structures of literature-known pyrrocorphins.

Scheme 1. Oxidation of OEP to the corresponding β -oxo-derivatives.⁹⁻¹⁰ Note that the hydroporphyrin nomenclature-based naming of the oxo-derivatives used here is descriptive of their architectures, but not their spectroscopic properties. Also shown is the framework numbering system used.



The general electronic influences of the β -oxo-substituents have been well-described within the realm of mono- and bis- β -oxo-substituted porphyrinoids (including the ketone functionalities of the porphalactones).^{9c,9d,11} These studies also revealed regiochemical influences and effects on the aromaticity parameters of the chromophores.^{9d,12} We recently presented work on all isomers of the pyrrocorphin β -triketones.¹⁰ We showed that they exhibit an aromatic macrocycle, expressed through a 16-membered, 18 π -macrocycle anion chromophore along a so-called inner-inner-inner-outer conjugation pathway, whereas all constitutional isomers of the triketones exhibit much different degrees of aromaticity.¹⁰ The chemistry of the mono- and diketones was explored to some extent;^{9,13} however, the

Arguably the synthetically simplest method to introduce β -oxo functionalities into β -alkylporphyrins is a one-pot epoxidation \rightarrow epoxide opening \rightarrow pinacol-pinacolone rearrangement sequence induced by their treatment with H_2O_2 in conc. H_2SO_4 (Scheme 1). Going back to classic work by the group of Fischer,⁷ the major product of the treatment of octa-ethylporphyrin OEP with $\text{H}_2\text{O}_2/\text{H}_2\text{SO}_4$ is 7-oxochlorin **5-O⁷**.⁸ The reaction can take place multiple times on the same macrocycle. Thus, chromatographic separation of the reaction mixture isolates all possible isomers of the β,β' -dioxo-derivatives (three isomers of the isobacteriochlorin series **6**; two isomers of the bacteriochlorin series **7**), and two (out of the four possible) triketone isomers **8**, as well as *meso*-oxo-substituted phlorins and ring-opened products.⁹ We recently presented a more directed synthesis of the remaining constitutional isomers of the triketones.¹⁰

Field Code Changed

chemistry of the β -triketones **8** was, aside from limited coordination chemistry studies,¹⁴ largely ignored.

We present here the regioselective reduction of one or two ketone functionalities of the two most common β -triketones, 2,7,12- and 2,7,18-trioxopyrrocorphins **8-O^{2,7,12}** and **8-O^{2,7,18}**. The crystal structures of select reduction products are reported. The reduction of the β -triketones is complemented by the OsO_4 -mediated dihydroxylation of select β -diketones, resulting in the synthesis of alternative mixed-pyrrole/pyrrolinone/pyrrolidine chromophores of equivalent electronic properties. The novel chromophores represent the redox-state intermediates between the classic non-aromatic pyrrocorphins and the aromatic pyrrocorphinketones. Their UV-vis and fluorescence spectra,

experimental and computational investigations of their diatropic ring currents, and halochromic properties provide clear evidence for the electronic influences of the β -oxo-substituents. In particular, the work provides evidence that all three β -oxo-substituents are needed to maintain the unique aromaticity of the pyrrocorphin triketones.

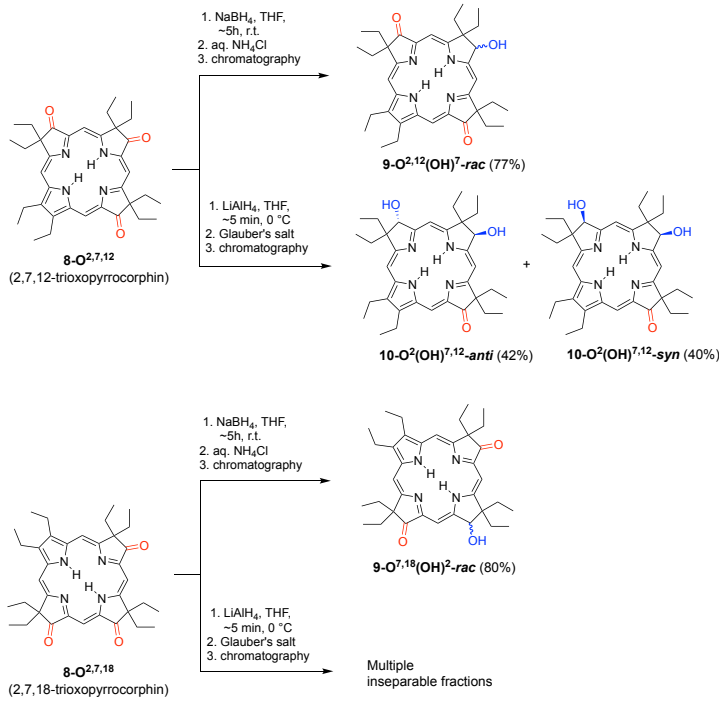
RESULTS AND DISCUSSION

Chemical Reduction of β -Trioxopyrrocorphins and the Optical Spectra of the Reduction Products

The regioselective reduction of one of the two ketone functionalities of the dioxo-chromophores **6-O** and **7-O** to the corresponding alcohols with NaBH_4 was previously shown to be possible.¹⁵ Likewise, we find now that the reduction of the pyrrocorphin trioxoisomers **8-O**^{2,7,12} or **8-O**^{2,7,18} with NaBH_4 over the course of several hours generates the mono-reduced

products **9-O**^{2,12(OH)^{7-rac} and **9-O**^{7,18(OH)^{2-rac}, respectively (Scheme 2). The presence of only a single diagnostic pyrroline hydrogen atom in the ¹H NMR spectra of both **9-O**^{2,12(OH)^{7-rac} and **9-O**^{7,18(OH)^{2-rac} is clear evidence that a regioselective mono-reduction had taken place. Similarly, the two carbonyl carbon signals in their ¹³C spectra indicate mono-reduction. Notably, upon reduction, the *meso*-protons appear in the ¹H NMR spectra of the product significantly upfield shifted compared to the position of the corresponding protons in the starting material (for a detailed discussion of the trends observed in the ¹H NMR spectra of the mixed-pyrrole/pyrrolinone/pyrroline chromophores, see below). The composition of the products, as determined by HR-ESI⁺ MS, also confirmed mono-reduction ($\text{C}_{36}\text{H}_{48}\text{N}_4\text{O}_3$ for M^+) (for details to the spectroscopic characterization of all new compounds, see SI). Single crystal X-ray diffractometry provided unambiguous evidence that the 'middle' -oxo-group was regioselectively reduced (see below).}}}}

Scheme 2. Mono- and bis-reductions of the tri-oxopyrrocphin isomers shown.



The UV-vis spectra of the mono-reduced products show significant blue-shifts (Figure 3). The observed reductions in extinction coefficients (for the non-normalized spectra, see SI) is contrary to the general trends observed upon the reduction of regular porphyrins or porpholactones.^{1b,1c} Both regioisomers show, as expected,^{15a,16} significant differences in their optical spectra. The reduced chromophores remain to be strongly emissive, with chlorin-like single emission bands, and the small Stokes shift typical of porphyrinoids.

When we subjected triketones **8-O**^{2,7,12} and **8-O**^{2,7,18} to 15 equiv. of LiAlH_4 , i.e., conditions we showed earlier to lead to

the bis-reduction of the β -diketones,^{15a} we saw differences in the outcome between the two regioisomers. The myriad of reduction products formed by reduction of **8-O**^{2,7,18} were intractable (even using smaller triketone to reductant stoichiometric ratios). However, those formed by reduction of **8-O**^{2,7,12} produced essentially only two readily separable polar fractions in unequal amounts. Both products possess identical optical spectra (see SI), identical compositions ($\text{C}_{36}\text{H}_{48}\text{N}_4\text{O}_3$ for M^+ , as per ESI⁺ HR-MS), similar but distinctly different ¹H NMR spectra (see SI) and show the presence of a single carbonyl carbon in their ¹³C NMR spectra (see SI). Thus, we conclude that only two out

of the three carbonyl groups were regioselectively reduced. The fractions were assigned to be the *syn*- (higher polarity product) and *anti*-diastereomers (lower polarity product) of the diols **10-O²-(OH)^{7,12}**, an interpretation confirmed by single crystal X-ray diffractometry (see below).

The ¹H NMR spectra of the bis-reduced products showed the hallmarks of the losses of macrocycle aromaticity (for a detailed description, see below). The UV-vis spectra of the bis-reduced

products were drastically blue-shifted compared to the spectra of the mono-reduced products (Figure 3), showing more similarity in peak shape and position to conjugated oligopyrroles than macrocycle-aromatic porphyrinoids.¹⁷

An attempt at increasing the stoichiometric excess of LiAlH₄ to beyond 15-fold to generate the tris-reduced systems led to the degradation of reactant/products, possibly a sign of the instability of the resulting ‘true’ pyrrocophins.

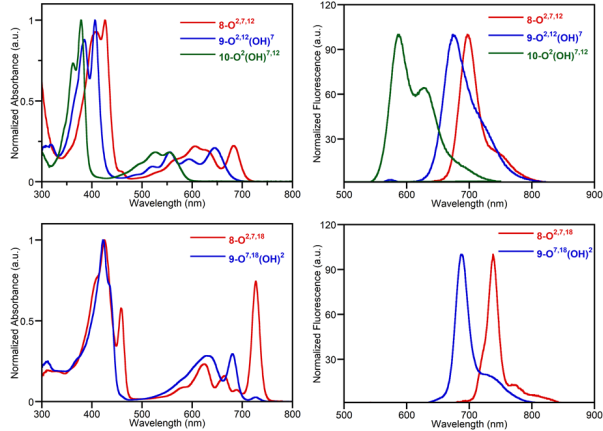


Figure 3. UV-vis (left) and fluorescence emission (right) spectra (CH_2Cl_2) of trioxopyrrocorphin **8-O^{2,7,12}** (top, red trace) and **8-O^{2,7,18}** (bottom, red trace) and their corresponding mono- (blue traces) (racemic mixture) and bis-reduced derivative (green trace) (*anti*-isomer).

Computations provide some indications for the origin of the regioselective reductions and the difference between the regioselectivities of the two triketone isomers. The reduction product of **8-O^{2,7,12}** in which the middle oxo group was reduced, was computed to result in the most thermodynamically favored of the three possible reduction products. Reduction of the 2-, 7-, or 12-positions gave ΔG_{rxn} of -0.05 -3.14, -2.80 kcal/mol, respectively (for details to the computations, see SI). Interestingly, the relative differences between the three regioisomeric reduction products of **8-O^{2,7,18}** show a much smaller

differentiation, with ΔG_{rxn} for the reduction at the 2-, 7-, and 18-positions of -2.79, -2.95, -2.10 kcal/mol, respectively.

Solid State Structures of the Mono- and Bis-reduced Trioxopyrrocorphin **8-O^{2,7,12}**

The solid-state structures of the mono-reduced (**9-O^{2,12}(OH)^{7-rac}**) and one diastereomer of the bis-reduced products (**10-O²(OH)^{7,12-anti}**) of triketone isomer **8-O^{2,7,12}** provide direct proof for the connectivity, regio- and stereochemistry of these products (Figure 4).

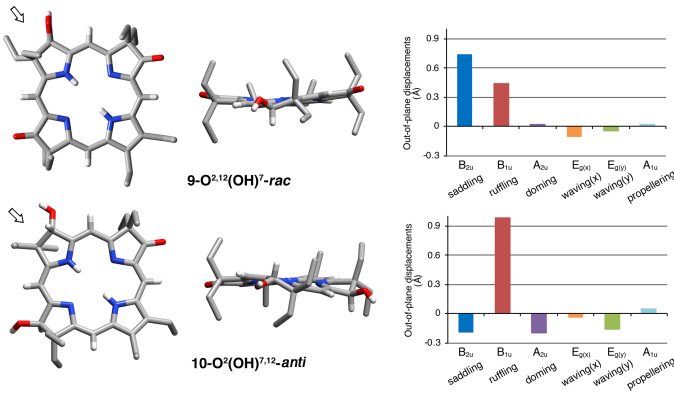


Figure 4. Stick representation of the X-ray single crystal structures of the compounds indicated, top and side views; the arrow in the top view images shows the point of view of the corresponding side view. All disorder and solvents (if present) are removed for clarity; all ethyl-hydrogen atoms were removed for clarity; for **9-O^{2,12}(OH)⁷-rac**, only one enantiomer of the racemic mixture present in the non-chiral unit cell shown. NSD analysis¹⁸ as implemented by Kingsbury and Senge.¹⁹ For details of the structural determinations and structural analyses, see SI.

Reduction of the β -oxo groups leads to a significantly and incrementally increased degree of non-planarity of the macrocycles, with modest ruffling and saddling modes for the mono-hydroxy compound **9-O^{2,12}(OH)⁷-rac** and significant ruffling for the bis-reduced analogue **10-O²(OH)^{7,12}-anti**. An increase of the conformational flexibility of the macrocycle is expected to be concomitant with increased framework carbon reductions.²⁰

Dihydroxylation of Dioxochlorin Isomers **6-O^{2,7}**, **6-O^{3,7}**, and **7-O^{7,17}** and Optical Properties of the Products

The reduction of the triketones generated a number of isomers of mixed-pyrrole/pyrrolinone/pyrrolidine macrocycles, but a full set of isomers would be desirable to derive a complete structure-optical properties relationship (Figure 5).

In an attempt to realize those isomers not accessible by reduction of the triketones, we chose to dihydroxylate the three

most readily available β -dioxo-derivatives.^{9c,9d} Thus, we applied the OsO₄-mediated dihydroxylation protocol developed for the conversion of octaethylporphyrin to dihydroxychlorins and tetrahydroxybacteriochlorins,^{13a} using 2 equiv. of OsO₄ to dioxoisobacteriochlorins **6-O^{2,7}** and **6-O^{3,7}** and dioxobacteriochlorin **7-O^{7,17}** (Scheme 3). This produced, as expected, the corresponding dioxo-osmate esters, as indicated by the diagnostic signals of osmium-coordinated pyridine moieties in their ¹H NMR spectra (see SI). The oxidation of **6-O^{3,7}** also resulted in the formation of a small portion of triketone isomer **8-O^{2,8,18}** (one of the rare isomers among the triketones).¹⁰ While it is tempting to assume that the product is the product of adventitious cleavage of the osmate ester/rearrangement of the diol, deliberate acid-induced rearrangement of the corresponding diol formed a different trioxopyrrocorphin isomer, namely **8-O^{2,7,18}** (see below).

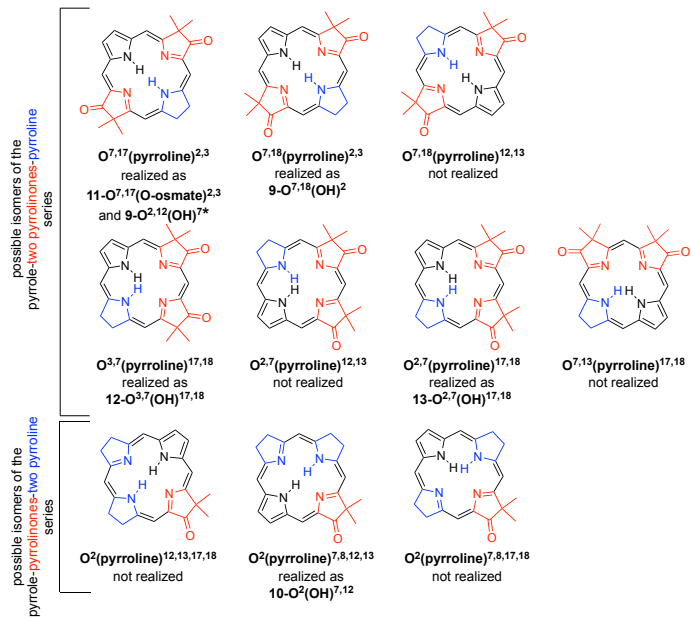
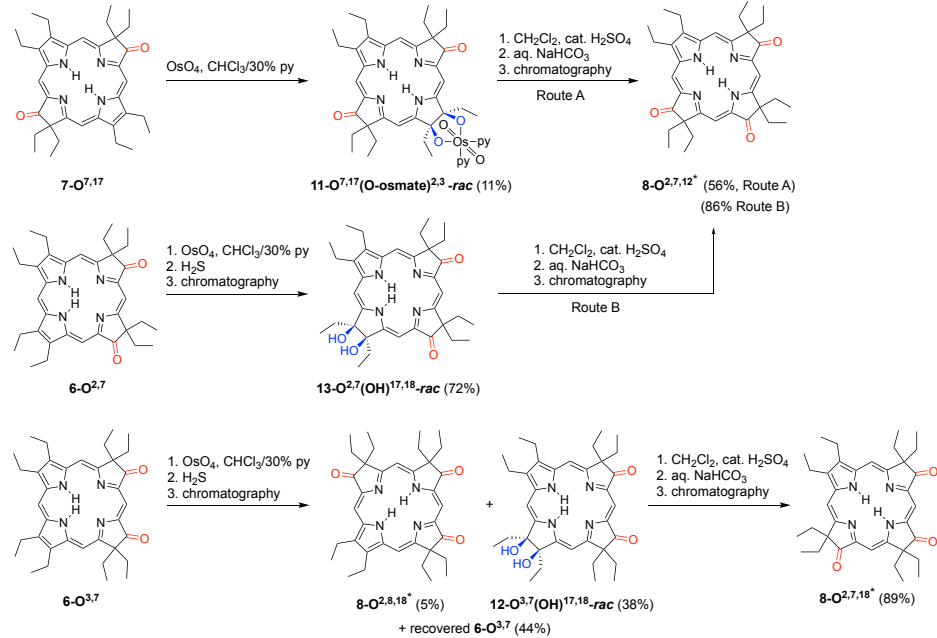


Figure 5. Representation of all isomers of the mixed pyrrole-pyrrolinone-pyrrolidine isomers containing three non-pyrrole building blocks, with an indication which chromophores were experimentally realized and which we have only computational data for (see below). * Note This chromophore uses a different numbering system than the same chromophore $11-O^{7,17}(\text{O-osmate})^{2,3}$ so to allow an orientation that highlights their origin from the parent chromophores (that each adhere to the numbering system shown in Scheme 1).

Scheme 3. Dihydroxylation of the β -dioxo-derivatives isomers shown and outcomes of the pinacol-pinacolone rearrangements of the resulting diols/diol osmate esters. * Note: The numbering chosen for the triketones is consistent with the prior literature¹⁰ and the system delineated in Scheme 1, except that the orientation of the molecule was chosen to highlight its genealogy.



Reduction of the osmate esters to the corresponding diols was performed using gaseous H₂S^{13a} generating the dihydroxylated products. Reduction of the osmate esters resulting from the osmylation of dioxobacteriochlorins 6-O^{2,7} and 6-O^{3,7} was smooth at ambient conditions, generating diols 13-O^{2,7}(OH)^{17,18}-rac and 12-O^{3,7}(OH)^{17,18}-rac, respectively. Diols 13-O^{2,7}(OH)^{17,18}-rac and 12-O^{3,7}(OH)^{17,18}-rac were characterized by the downfield shift of their inner NH protons in their ¹H NMR spectra, compared to the spectra of the corresponding diketones (for more details, see below). Mass spectrometry confirmed them to have the expected composition (C₅₆H₄₄N₄O₃ for M⁺, as per ESI⁺-HR-MS). On the contrary, the osmate ester of the dihydroxylated dioxobacteriochlorin, 11-O^{7,17}(O-osmate)^{2,3}-rac was unexpectedly (and inexplicably) robust; we could not prepare the diol under the standard conditions. As observed before, the osmate esters are not susceptible to characterization using ESI⁺ mass spectrometry; they inevitably lose the osmate ester and show the mass signal for the diol only (see SI).²¹

The dehydroxylated or osmylated chromophores of the dioxo-derivatives show UV-vis spectra of aromatic porphyrinoid character (Figure 6). They feature, in comparison of their corresponding dioxo and triketones, distinct split Soret bands with hypsochromic shifts and well-defined side bands.

Their position generally matches the positions of the side bands of the corresponding triketone isomers. Again, the fluorescence spectra of dihydroxy- β -dioxo-derivatives are typical for hydroporphyrins in that they show a single band, also largely resembling the emission spectra of the corresponding triketone isomers. The emission spectrum of the osmate ester 11-O^{7,17}(O-osmate)^{2,3}-rac shows only negligible fluorescence (see SI).

Several observations are important: The spectra of the two compounds 11-O^{7,17}(O-osmate)^{2,3} (Figure 6) and 9-O^{2,12}(OH)⁷ (Figure 3) are near-identical to each other (for a direct overlay, see Figure S49). Thus, they possess equivalent chromophore though the pyrrole moiety was realized in two different ways (dihydroxylation of a pyrrole moiety or reduction of a pyrrolinone, respectively). The minimal influence of the β,β' -diol functionality when compared to the mono- β -hydroxyhydroporphyrin or parent unsubstituted hydroporphyrin was observed before.²² This is the basis for the modeling of the mono-hydroxylated chromophores to also realistically represent the spectra of the dihydroxylated analogues (or their hydroxy-free analogues). On the other hand, the regiochemical influences of the β -oxo-group on the UV-vis absorption and fluorescence emission spectra are stark.

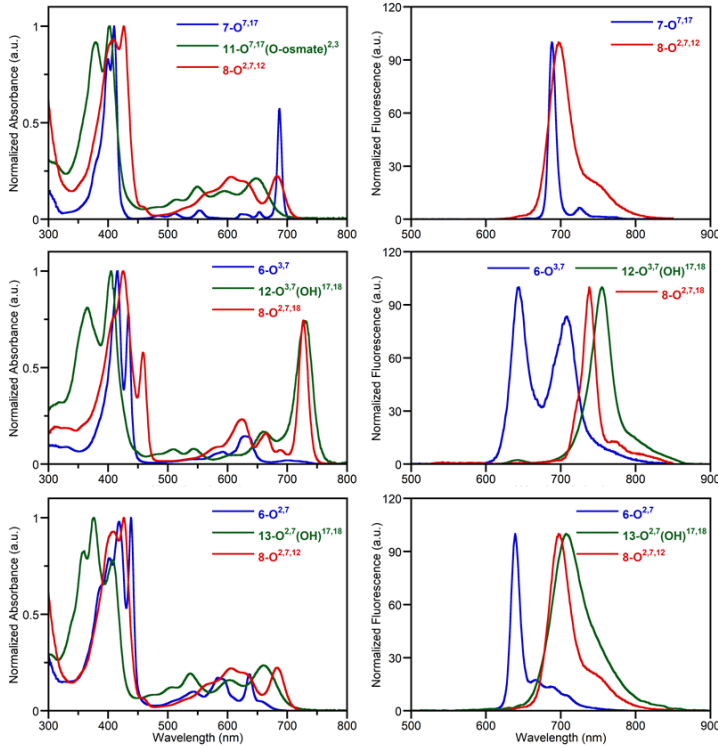


Figure 6. UV-vis (left) and fluorescence emission (right) spectra (CH_2Cl_2) of dihydroxylated dioxo chromophores (green), their corresponding dioxo (blue traces), and trioxo- derivative (red traces) as indicated. Emission spectrum for **11-O^{7,17}(O-*osmate*)^{2,3}-rac** is not shown due to its negligible fluorescence (see SI).

¹H NMR Spectroscopic Comparison of the Trioxo-pyrrocorphins and their Reduced Chromophores

In general, the NMR spectra of all reduced products show the low-field singlets diagnostic for their *meso*-CH protons, the pyrroline hydrogen atoms in the region between 4 and 6 ppm, and the alkyl protons (with some methylene protons of the *gem*-diethyl group neighbouring a ketone group clearly identifiable by their low-field shift signals). The exchangeable protons of the OH- (were present) and NH-groups were also confirmed by D_2O exchange experiments. For further details, see SI.

In comparison to the *meso*-CH signals of the dioxo- and trioxochromophores (Figure 7),^{9b-d,10} the corresponding signals for the dihydroxylated dioxo-chromophore and reduced trioxopyrrocorphins are shifted upfield, while the NH signals are particularly shifted downfield at the same time. This trend is more pronounced with an increase in the number of pyrroline building blocks. The gap between the diatropic shifts of the hydrogens inside and outside the aromatic macrocyclic π -system, expressed as $\Delta\delta_{\text{NH}-\text{meso}}$, averages 3.8 or 3.9 ppm for the pyrrole-two pyrrolinone-pyrroline chromophores (for dihydroxylated dioxopyrrocorphin product **13-O^{2,7}(OH)^{17,18}-rac** and the mono-

reduced triketone **9-O^{2,12}(OH)⁷-rac**, respectively), whereas this gap is even much more narrow (1.4 ppm) in the bis-reduced triketone **10-O^{2(OH)^{7,12}}**. In comparison, this gap is significantly wider (6.3 and 9.0 ppm) for the corresponding weakly aromatic triketone **8-O^{2,7,12}** and the fully aromatic diketone **6-O^{2,7}**, respectively. We interpret this closing of $\Delta\delta_{\text{NH}-\text{meso}}$ as a reduction of the degree of aromaticity of the mixed-pyrrole/pyrrolinone/pyrroline macrocycles,¹⁰ with the bis-reduced triketone **10-O^{2(OH)^{7,12}}** being essentially non-macrocycle aromatic.

Since the macrocycles are all believed to be planar (as shown for some, see above) we surmise that the internal H-bond patterns are not altered drastically among the compounds studied (accordingly, the crystal structures support this, also). Consequently, we can exclude these effects as alternative interpretations of the observed drastic NH shifts. The chemical shifts of the *meso*- and NH protons and, consequently, the experimental $\Delta\delta_{\text{NH}-\text{meso}}$ values, are also in good agreement with those reported for other β -alkylpyrrocorphins.²³ Finally, the values are also in excellent agreement with the computed values using structures with essentially unaltered internal H-bond patterns (see below).

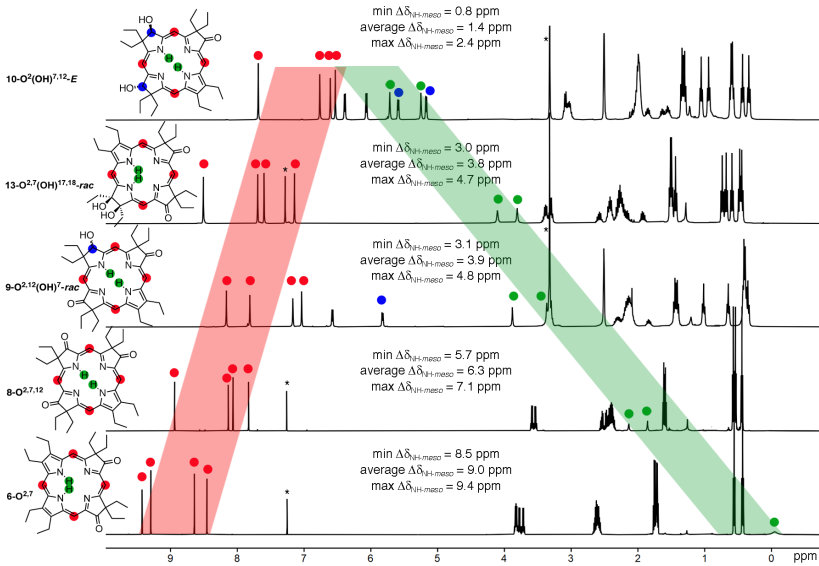


Figure 7. Comparison of the ^1H NMR spectra (400 MHz, 20 °C, CDCl_3 , except for $9\text{-O}^{2,12}(\text{OH})^7\text{-rac}$ and $10\text{-O}^2(\text{OH})^{7,12}\text{-anti}$, DMSO-d_6 was used; residual solvent peaks indicated with *) of the compounds indicated, highlighting the trends of the shifts for the *meso*-protons (red) and the NH protons (green). The changes in diatropicity are indicated as $\Delta\delta_{\text{NH-meso}}$, the difference in the chemical shifts of the *meso*- and inner NH protons. For details, see SI.

Computed Optical Spectra and Aromaticity Parameters of All Mixed Pyrrole-Pyrrolinone-Pyrrolidine Macrocycles

We performed ground and excited electronic state density functional theory (DFT) computations (BHandHLYP with either def2-SVP or def2-TZVP for geometry optimizations and response properties, respectively; for details, see SI)²⁴ of all isomers of the mixed-pyrrole/pyrrolinone/pyrrolidine macrocycles to further shed insight onto the origin of their optical spectra and aromaticity parameters, particularly for those isomers that could not be prepared (Figure 8; cf. to Figure 5). The computed UV-vis spectra of the two triketone isomers **8-O^{2,7,12}** and **8-O^{2,7,18}** and the corresponding regioisomers of the mono- and bis-, and tris-reduced pyrrocorphins show the impact of increasing conversions of pyrrolinones to pyrrolines and the strong regiochemical influence of the β -oxo moieties on the electronic structure of the isomers within a given reduction state. Since the spectra match the experimental data well, we are confident that

the computed spectra of the unrealized chromophores are realistic predictions.

The three different regioisomers of the monoreduced derivatives of triketone **8-O^{2,7,12}** show comparably fewer differences than the monoreduced derivatives of triketone **8-O^{2,7,18}**, which exhibit considerable shifts (up to 70 nm for λ_{max} , for example). The situation is slightly different for the bis-reduced series: Some isomers in both the **8-O^{2,7,12}**- and **8-O^{2,7,18}**-derived series are similar to each other, while others are much different from each other (such as the spectrum of **O^{2(OH)^{7,12}}** when compared to that of **O^{2(OH)^{7,18}}**). The spectra of the tris-reduced derivatives of both triketone isomers (**O^{2(OH)^{2,7,12}}** and **O^{2(OH)^{2,7,18}}**) are near-identical, are much hypsochromically shifted and typical for the non-macrocyclic-aromatic pyrrocorphins. The near-identical spectra again highlight that only the β -oxo-functionalities have a strong regiochemical influence, as shown previously for a series of porpholactones/oxazolochlorins.^{12,25}

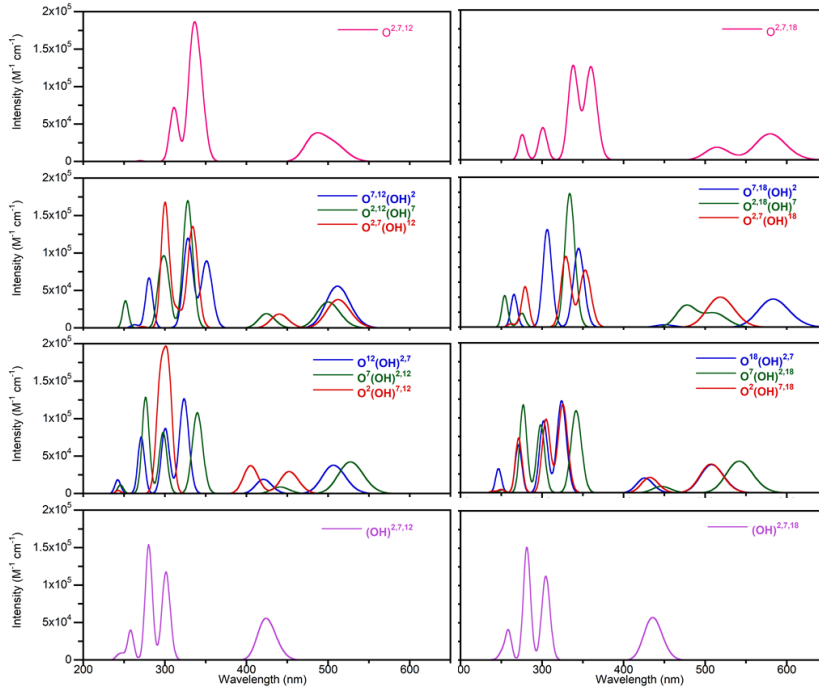


Figure 8. Comparison of the computed UV-vis spectra for the triketone (top) isomers **8-O^{2,7,12}** (left) and **8-O^{2,7,18}** (right), the corresponding regioisomers of the monoreduced (second row) and bisreduced (third row), and the trisreduced pyrrocorphins (bottom row).

The $\Delta\delta_{\text{NH}-\text{meso}}$ values of all possible isomers of the **8-O^{2,7,12}**- and **8-O^{2,7,18}**-derived series were also analyzed computationally (BHandHLYP/def2-TZVP, for details, see SI) with the benefit that these aromaticity parameters could be experimentally verified, as opposed to other popular aromaticity parameters, such as NICS values, ACID plots, or GIMIC ring current susceptibilities (Figure 9).²⁶ The computed $\Delta\delta_{\text{NH}-\text{meso}}$ agreed very well with the experimental data for the compounds that could be experimentally prepared (cf. also to Figure 7).

The bar diagram highlights two findings: For one, the rapid degradation of the $\Delta\delta_{\text{NH}-\text{meso}}$ values with increasing reduction and the large differences between the compounds derived from the **8-O^{2,7,12}**- and **8-O^{2,7,18}**-series, with those derived from **8-O^{2,7,18}** possessing consistently larger $\Delta\delta_{\text{NH}-\text{meso}}$ values and, thusly, larger degrees of aromaticity.

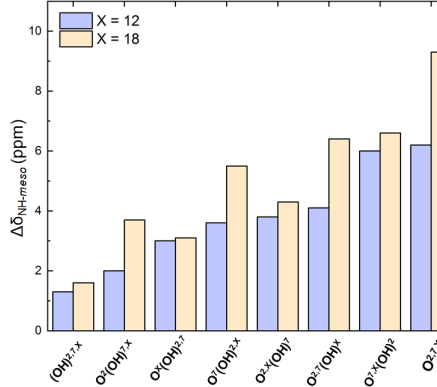


Figure 9. Computed chemical shift difference values $\Delta\delta_{\text{NH}-\text{meso}}$ between inner NH and outer *meso*-proton resonances of the triketones (**O^{2,7,X}** where $X = 12, 18$) and the different regioisomers of their corresponding mono- (**O^{¹(y)pyrroline}**)^², bis- (**O^{¹(y)pyrroline}**)^¹, and tris-reduced species (**O^{¹(y)pyrroline}**)^{²,7,X} where $X = 12, 18$ chromophores.

Halochromic Properties of the Reduced Trioxopyrrocophins

One experimental evidence that supported the presence of the 16- π , 18-membered dianionic π -system in the trioxoketones was their unusual susceptibility to base.¹⁰ For example, upon addition of the base tri-*n*-butylammonium hydroxide (TBAOH) (in MeOH) to a solution of **8-O^{2,7,12}** in CH₂Cl₂, its UV-vis spectrum intensified and shifted significantly (Figure 10). This halochromic response to base is unusual for regular (hydro)porphyrins not containing an acidic macrocycle substituent.

To determine the effects of the replacement of one or two of the pyrrolidones in trioxopyrrocophins by β -hydroxylated

pyrrolines on the halochromic response to base, we added a solution of TBAOH to, for example, **9-O^{2,12}(OH)^{7-rac}**, **10-O^{2(OH)^{7,12-anti}}**, or **12-O^{2,7(OH)^{17,18-rac}}** (for additional examples, see SI). Unlike, the distinct and drastic response of the triketones, none of the β -hydroxylated di- and mono-ketones showed any indication for the loss of inner core imine protons; they either showed no (beyond dilution effects) or only minor general shifts, possibly indicative of an onset of the deprotonation of the β -hydroxy groups. Their response to the addition of acid (TFA) is as complex as that of the triketones (see SI).

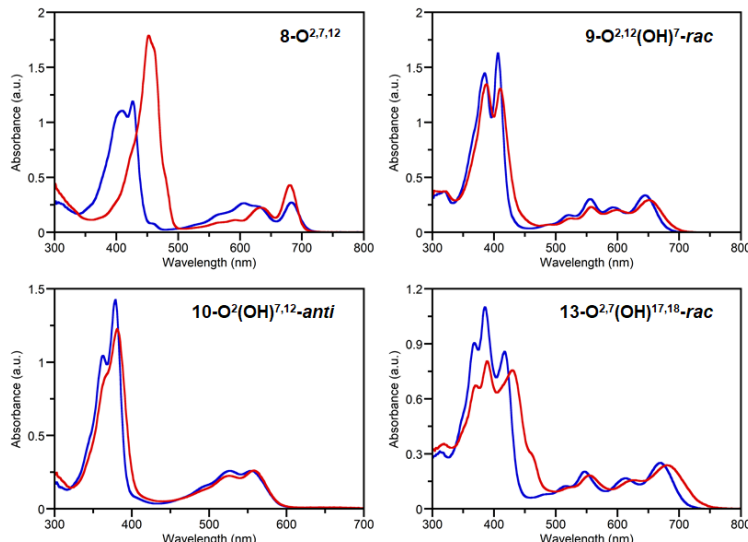


Figure 10. UV-vis spectra of the compounds indicated before (CH₂Cl₂, blue traces) and after addition of tri-*n*-butylammonium hydroxide (TBAOH) (CH₂Cl₂ + 1 M TBAOH in MeOH, red traces). TBAOH solution was added to a sample until no further shift was observed while keeping the dilution errors < 2%.

Acid-induced Rearrangement of the Dihydroxy-dioxopyrrocophins

Treatment of dihydroxy-dioxopyrrocophins **13-O^{2,7(OH)^{17,18-rac}}** or **11-O^{7,17(O-^{2,3}-osmate)^{2,3-rac}}** with catalytic amount of H₂SO₄ in CH₂Cl₂ generated the triketone isomer **8-O^{2,7,12}** (Scheme 3). Equivalent treatment of diol **12-O^{3,7(OH)^{17,18-rac}}** generated the trioxopyrrocophin isomer **8-O^{2,7,18}**. Both trioxopyrrocophin isomers are the most common triketone isomers that are also formed by direct oxidation of **OEP**.^{9b,10} Curiously, the trioxopyrrocophin isomer **8-O^{2,7,18}** formed via the acid-induced rearrangement of **12-O^{3,7(OH)^{17,18-rac}}** is a different isomer than trioxopyrrocophin **8-O^{2,8,18}** found as a side product during the oxidation of dioxochromophore **6-O^{3,7}** (see also above). We surmise these two trioxopyrrocophins were formed along different reaction trajectories.

Overall, the step-wise syntheses of the triketones is preferable over the bulk oxidation of **OEP** and the subsequent chromatographic separation; the yields are overall higher and larger quantities can be more readily prepared.^{9b,10}

CONCLUSIONS

In conclusion, two β -trioxopyrrocophin isomers could be regioselectively mono-reduced and one of the isomers bis-reduced. Some stereoisomers could be separated. More isomers of the mixed pyrrole/pyrrolidine/pyrrolone chromophores could be prepared by osmium tetroxide-mediated dihydroxylation of β -dioxo-substituted chromophores. All are believed to be only minimally distorted from planarity (shown for two compounds by single crystal X-ray crystallography). Thus, the electronic differences between the compounds are largely attributed to electronic substituent effects rather than being conformationally induced. All isomers and reduction states showed distinctly different optical (UV-vis and fluorescence) spectra. Generally, with increasing reduction, the graded aromatic character of the pyrrocophins deteriorates and is essentially lost in the tris-reduced, regular pyrrocophins. The loss of aromaticity was primarily traced by the loss of diatropic shifts of inner and outer framework proton signals in their ¹H NMR spectra. We also computed the optical spectra and aromaticity parameters of all possible isomers of the mono- and bis-reduction states of the **8**

O^{2,7,12}- and 8-O^{2,7,18} triketone pyrrocorphin-derived series. An excellent match with the experimental data was observed.

The difference in the absorption spectra and aromaticity parameters of the different reduction states and regioisomers of a given reduction state provides another set of clear evidence of the impact of the number and position of the β -oxo-auxochromes on the conjugation pathway and electronics of the porphyrinic chromophores. We could not discern a classic conjugation pathway-based rationalization of the enormous influence of the position of the β -oxo-substituents on the electronic properties of these mixed single pyrrole-pyrrolinone-pyrrolidine chromophores. The work increases the knowledge of pyrrocophins, a family of less studied hexahydroporphyrins, particularly those of an oxidation state between the trioxopyrrocophins and the classic non-carbonylated pyrrocophins.

Thus, this work contributes further insights into the electronic structure of the β -oxoporphyrinoids and expands the toolset for the precise modulation of porphyrinoid electronic properties by systematically varying the number and relative orientation of β -oxo-substituents in mixed pyrrole-pyrrolinone-pyrrolidine chromophores. The work increases the knowledge of pyrrocophins, a family of less studied hexahydroporphyrins, particularly those of an oxidation state between the trioxopyrrocophins and the classic non-carbonylated pyrrocophins.

EXPERIMENTAL SECTION

Materials

Solvents and reagents were used as received. Aluminum-backed, silica gel 60, 250 μ m thickness analytical plates, 20 \times 20 cm, glass-backed, silica gel 60, 500 μ m thickness preparative TLC plates, and standard grade, 60 \AA , 32-63 μ m flash column silica gel were used for purifications.

β -Dioxoderivatives (**6-O^{2,7}**, **6-O^{3,7}** and **7-O^{7,17}**) and trioxopyrrocophins **8-O^{2,7,12}** and **8-O^{2,7,18}** were prepared from OEP (2 g, 3.74 \times 10⁻³ mol) in H₂SO₄ (200 mL) with 3% H₂O₂ (36 mL) as described by Inhoffen and Nolte or Chang,^{9b,9c} and recently reproduced and expanded by us.^{9d,10}

Procedures

General Procedure for the Preparation of Hydroxydioxochromophores 9 by Mono-Reduction of Triketones 8-O^{2,7,12} or 8-O^{2,7,18}. A solution of trioxopyrrocophins **8-O^{2,7,12}** or **8-O^{2,7,18}** (50 mg, 8.58 \times 10⁻⁵ mol) in THF (2.0 mL) was stirred under N₂ on an ice bath for several minutes. To the chilled solution were added 5 equiv. of NaBH₄ (17 mg, 4.29 \times 10⁻⁴ mol) and the reaction mixture was stirred for ~4-5 h at ambient temperature. After all starting material was consumed (TLC), the reaction mixture was diluted with CH₂Cl₂ (20 mL) and washed with a sat'd aqueous solution of NH₄Cl. The organic layer was separated, dried over anhydrous Na₂SO₄, and filtered. The filtrate was reduced to dryness using rotatory evaporation. The crude mixture was purified by silica-gel column chromatography.

3,3,8,8,13,13,17,18-Octaethyl-7-hydroxy-2,12-dioxopyrrocorphin (9-O^{2,7,12(OH)}-rac). Prepared by reduction of **8-O^{2,7,12}** (50 mg, 8.58 \times 10⁻⁵ mol) with NaBH₄ (17 mg, 4.29 \times 10⁻⁴ mol, 5 equiv.) in THF (2.0 mL) following the general procedure. The product was isolated as a blue solid in 77% yield (38.5 mg, 6.58 \times 10⁻⁵ mol). Preparative TLC conditions: hexanes-CH₂Cl₂ (30:70 v/v) followed by 100% CH₂Cl₂. MW = 584.79 g/mol; R_f = 0.22 (silica-CH₂Cl₂). ¹H NMR (400 MHz, CDCl₃): δ 8.15 (s, 1H), 7.80 (s, 1H), 7.16 (s, 1H), 7.03 (s, 1H), 6.57 (d, $^3J_{\text{HH}} = 6.5$ Hz, 2H), 5.81 (d, $^3J_{\text{HH}} = 6.5$ Hz, 2H), 3.87 (s, 1H), 3.36 (s, 1H), 3.34-3.27 (m, 4H), 2.33-2.08 (m, 11H), 1.89-1.78 (m, 1H), 1.42 (dt, $^3J_{\text{HH}} = 14.5$, 7.5 Hz, 6H), 1.01 (t, $^3J_{\text{HH}} = 7.5$ Hz, 3H), 0.64 (t, $^3J_{\text{HH}} = 7.0$ Hz, 3H), 0.43-0.33 (m, 12H) ppm. ¹³C{¹H} NMR (101 MHz, CDCl₃): δ 208.3, 207.5, 170.3, 155.5, 153.9, 152.0, 141.1, 134.3, 132.0, 131.1, 127.6, 99.4, 99.2, 88.8, 84.6, 76.9, 59.6, 55.6, 53.6, 30.3, 30.0, 29.3, 29.3, 28.5, 26.9, 17.8, 17.6, 17.5, 8.8, 8.5, 8.3, 8.2 ppm. UV-vis (CH₂Cl₂) λ_{max} (log ϵ): 384 (5.05), 406 (5.11), 519 (4.08), 554 (4.37), 593 (4.25), 645 (4.43) nm; fluorescence (CH₂Cl₂, $\lambda_{\text{excitation}} = 400$ nm) $\lambda_{\text{max-emission}} = 675$ nm; IR (diamond ATR, neat): 1690 (v_{C=O}), 3304, 3397 (v_{N-H}) cm⁻¹. HR-MS (ESI⁺, 100% CH₃CN, TOF): calc'd for C₃₆H₄₈N₄O₃ [M]⁺ 584.3726, found 584.3664.

3,3,8,8,12,13,17,17-Octaethyl-2-hydroxy-7,18-dioxopyrrocorphin (9-O^{7,18(OH)}-rac). Prepared by reduction of **8-O^{2,7,18}** (50 mg, 8.58 \times 10⁻⁵ mol) with NaBH₄ (17 mg, 4.29 \times 10⁻⁴ mol, 5 equiv.) in THF (2.0 mL) according to the general procedure. The product was isolated as a green solid in 80% yield (40 mg, 6.84 \times 10⁻⁵ mol). Preparative TLC conditions: hexanes-CH₂Cl₂ (20:80 v/v). MW = 584.7913 g/mol; R_f = 0.14 (silica-CH₂Cl₂). ¹H NMR (400 MHz, CDCl₃): δ 8.11 (d, $^3J_{\text{HH}} = 5.0$ Hz, 2H), 8.00 (s, 1H), 7.65 (s, 1H), 6.01 (d, $^3J_{\text{HH}} = 6.5$ Hz, 1H), 3.54 (q, $^3J_{\text{HH}} = 7.5$ Hz, 4H), 2.44-2.31 (m, 10H), 2.24-2.15 (m, 2H), 1.79 (s, 1H), 1.61 (t, $^3J_{\text{HH}} = 7.5$ Hz, 6H), 1.28 (s, 1H), 1.03 (t, $^3J_{\text{HH}} = 7.5$ Hz, 3H), 0.96 (t, $^3J_{\text{HH}} = 7.5$ Hz, 3H), 0.52 (q, $^3J_{\text{HH}} = 7.0$ Hz, 12H) ppm. ¹³C{¹H} NMR (101 MHz, CDCl₃): δ 209.5, 209.3, 154.6, 154.6, 153.0, 152.9, 152.4, 147.0, 133.5, 133.3, 131.4, 131.3, 98.9, 98.4, 87.0, 86.9, 80.3, 57.5, 57.4, 54.6, 31.6, 31.4, 29.3, 25.5, 18.9, 18.3, 9.4, 9.0, 8.7 ppm. UV-vis (CH₂Cl₂) λ_{max} (log ϵ): 422 (4.69), 631 (4.15), 680 (4.16), 727 (3.12) nm. Fluorescence (CH₂Cl₂, $\lambda_{\text{excitation}} = 422$ nm) $\lambda_{\text{max-emission}} = 687$ nm. IR (diamond ATR, neat): 1711 (v_{C=O}), 3301, 3390 (v_{N-H}) cm⁻¹. HR-MS (ESI⁺, 100% CH₃CN, TOF): calc'd for C₃₆H₄₈N₄O₃ [M]⁺ 584.3726, found 584.3680.

Bis-reduction of Triketone 8-O^{2,7,12}. Trioxopyrrocophin **8-O^{2,7,12}** (80 mg, 1.37 \times 10⁻⁴ mol) was dissolved in dry THF (2.0 mL) and stirred on an ice bath under a dry N₂ atmosphere. To the chilled solution was added a suspension of LiAlH₄ (78 mg, 2.05 \times 10⁻³ mol, 15 equiv.) in THF (1 mL) and the mixture was stirred for ~3-5 min at 0 °C. The reaction was monitored by TLC and UV-vis spectroscopy. After completion of the reaction, the reaction mixture was quenched by slurrying with Glauber's salt (Na₂SO₄ 10 H₂O, ~1.5 g). The resulting mixture was filtered through a pad of Celite® and the pad was washed with CH₂Cl₂. The combined filtrates were passed through anhydrous Na₂SO₄ and reduced to dryness by rotatory evaporation. The crude solid was purified by either column or preparative plate chromatography.

3,3,8,8,13,13,17,18-Octaethyl-1,7,12-dihydroxy-2-oxopyrrocorphin (10-O^{2(OH)}-rac-anti). Isolated as a magenta crystalline solid in 42% yield (34 mg, 5.79 \times 10⁻⁵ mol). Chromatography conditions: separation on silica gel preparative TLC plate with 1% acetone in CH₂Cl₂. MW = 586.807 g/mol. R_f = 0.19 (silica-1% acetone in CH₂Cl₂). ¹H NMR (400 MHz, CDCl₃): δ 7.68 (s, 1H), 7.66 (s, 1H), 6.60 (s, 1H), 6.52 (s, 1H), 6.38 (d, $^3J_{\text{HH}} = 6.0$ Hz, 1H), 6.06 (d, $^3J_{\text{HH}} = 6.5$ Hz, 1H), 5.71 (s, 1H), 5.52 (d, $^3J_{\text{HH}} = 6.0$ Hz, 1H), 5.24 (s, 1H), 5.16 (d, $^3J_{\text{HH}} = 6.5$ Hz, 1H), 3.11-2.99 (m, 4H), 2.05-1.94 (m, 9H), 1.85 (dd, $^3J_{\text{HH}} = 13.5$, 7.0 Hz, 1H), 1.64-1.52 (m, 2H), 1.30 (dd, $^3J_{\text{HH}} = 15.0$, 7.5 Hz, 6H), 1.04 (t, $^3J_{\text{HH}} = 7.5$ Hz, 3H), 0.93 (t, $^3J_{\text{HH}} = 7.5$ Hz, 3H), 0.59 (dd, $^3J_{\text{HH}} = 16.5$, 7.5 Hz, 6H), 0.43 (t, $^3J_{\text{HH}} = 7.5$ Hz, 3H), 0.33 (t, $^3J_{\text{HH}} = 7.5$ Hz, 3H) ppm. ¹³C{¹H} NMR (101 MHz, CDCl₃): δ 206.7, 174.5, 169.5, 158.8, 155.1, 152.0, 139.2, 133.7, 132.0, 126.9, 124.5, 101.2, 97.1, 89.5, 87.5, 80.2, 76.0, 59.4, 53.4, 52.7, 29.2, 29.1, 28.5, 28.5, 27.7, 17.6, 17.5, 17.3, 9.4, 9.2, 8.8, 8.4, 8.3 ppm. UV-vis (CH₂Cl₂) λ_{max} (log ϵ): 362 (4.84), 378 (4.97), 525 (4.23), 554 (4.23) nm; fluorescence (CH₂Cl₂, $\lambda_{\text{excitation}} = 378$ nm) $\lambda_{\text{max}} = 587$, 628 nm. IR (diamond ATR, neat): 1666 (v_{C=O}), 3315, 3396 (v_{N-H}) cm⁻¹. HR-MS (ESI⁺, 100% CH₃CN, TOF): calc'd for C₃₆H₅₀N₄O₃ [M]⁺ 586.3883, found 586.3810.

3,3,8,8,13,13,17,18-Octaethyl-7,12-dihydroxy-2-oxopyrrocorphin (10-O^{2(OH)}-rac-syn). Prepared as a magenta crystalline solid in 40% yield (32 mg, 5.45 \times 10⁻⁵ mol). Chromatography condition: separation on preparative TLC plate with 1% acetone in CH₂Cl₂. MW = 586.8072 g/mol. R_f = 0.14 (silica-2% acetone in CH₂Cl₂). ¹H NMR (400 MHz, CDCl₃): δ 7.73 (s, 1H), 6.83 (s, 1H), 6.67 (s, 1H), 6.60 (s, 1H), 6.33 (d, $^3J_{\text{HH}} = 5.0$ Hz, 1H), 6.04 (d, $^3J_{\text{HH}} = 6.5$ Hz, 1H), 5.48 (s, 1H), 5.45 (d, $^3J_{\text{HH}} = 3.5$ Hz, 1H), 5.13 (d, $^3J_{\text{HH}} = 6.0$ Hz, 1H), 4.95 (s, 1H), 3.13-3.02 (m, 4H), 2.02-1.64 (m, 10H), 1.78 (dd, $^3J_{\text{HH}} = 14.0$, 7.5 Hz, 1H), 1.64 (dd, $^3J_{\text{HH}} = 14.0$, 7.0 Hz, 1H), 1.33 (dd, $^3J_{\text{HH}} = 16.0$, 8.0 Hz, 6H), 0.96 (t, $^3J_{\text{HH}} = 7.5$ Hz, 3H), 0.87 (d, $^3J_{\text{HH}} = 7.0$ Hz, 3H), 0.74 (t, $^3J_{\text{HH}} = 7.0$ Hz, 3H), 0.66 (t, $^3J_{\text{HH}} = 7.0$ Hz, 3H), 0.38 (t, $^3J_{\text{HH}} = 7.5$ Hz, 6H) ppm. ¹³C{¹H} NMR (101 MHz, CDCl₃): δ 206.7, 173.3, 169.5, 159.5, 155.4, 151.6, 139.2, 133.8, 132.0, 124.6, 101.0, 97.2, 89.7, 88.0, 80.8, 76.4, 59.4, 52.9, 52.6, 29.7, 29.1, 28.2, 28.0, 26.3, 17.6, 17.5, 17.3, 9.4, 9.0, 8.7, 8.6, 8.4, 8.3 ppm. UV-vis (CH₂Cl₂) λ_{max} (log ϵ): 362 (4.64), 379 (4.78), 525 (4.03), 554 (4.03) nm; fluorescence (CH₂Cl₂, $\lambda_{\text{excitation}} = 379$ nm) $\lambda_{\text{max}} = 588$, 630 nm; IR (diamond ATR,

neat): 1673 (v_{C=O}), 3305, 3388 (v_{N-H}) cm⁻¹. HR-MS (ESI+, 100% CH₃CN, TOF): calc'd for C₃₆H₅₀N₄O₃ [M]⁺ 586.3883, found 586.3864.

General Procedure for the Dihydroxylation of Dioxochlorins (6-O^{2,7}, 6-O^{3,7}, 7-O^{7,17}). Dioxochlorin (100 mg, 1.67 × 10⁻⁴ mol) was dissolved in a round bottom flask equipped with a stir bar in CHCl₃ and pyridine (7.3, v/v). The mixture was treated with 2 equiv. (3.34 × 10⁻⁴ mol) of OsO₄ (stock solution made of 1.0 g OsO₄ dissolved in 20 mL of pyridine). The reaction flask was stoppered, protected from light with aluminum foil, and stirred at ambient temperature. The appearance of the product was monitored by TLC and UV-vis spectroscopy. After ~24 h, once no further progress was observed in the reaction and the solvent was purged with H₂S for 2-3 minutes. The reaction mixture was filtered through a short plug of diatomaceous earth (Celite). The solvent was then removed to dryness by rotary evaporation. A gentle stream of N₂ for several hours ensured that the crude product was thoroughly dried before it was purified via flash chromatography (silica-CH₂Cl₂/1.0-5.0% acetone).

3,3,8,8,12,13,17,18-Octaethyl-17,18-dihydroxy-2,7-dioxopyrrocorphins (13-O^{2,7}(OH)^{7,18}-rac). Prepared by osmylation of dioxoisobacteriochlorin **6-O^{2,7}** as a purple solid in 72% yield (72 mg, 1.19 × 10⁻⁴ mol) according to the general procedure. About 10-15% (10–15 mg) of the starting material **6-O^{2,7}** was recovered from the column as the first fraction. Chromatography conditions for the product: CH₂Cl₂ followed by 5% acetone in CH₂Cl₂, MW = 600.804 g/mol, R_f = 0.71 (silica- 10% acetone in CH₂Cl₂). ¹H NMR (400 MHz, CDCl₃): δ 8.86 (d, ³J_{H,H} = 8.7 Hz, 2H), 8.69 (d, ³J_{H,H} = 10.9 Hz, 2H), 8.43 (s, 1H), 7.88 (s, 1H), 7.74 (s, 1H), 7.65 (d, ³J_{H,H} = 4.5 Hz, 2H), 7.48 (d, ³J_{H,H} = 9.0 Hz, 2H), 7.35 (s, 2H), 7.05 (s, 1H), 3.61 (s, 1H), 3.41 – 3.31 (m, 4H), 3.20 (s, 1H), 2.95 – 2.81 (m, 2H), 2.71 – 2.61 (m, 2H), 2.31 – 2.15 (m, 8H), 1.53 – 1.46 (m, 9H), 0.92 (t, ³J_{H,H} = 7.4 Hz, 3H), 0.58 – 0.42 (m, 12H). ¹³C{¹H} NMR (101 MHz, CDCl₃): δ 209.7 (C=O), 209.4 (C=O), 169.6, 155.4, 154.6, 152.4, 152.2, 150.8, 149.7, 142.8, 142.1, 135.1, 131.9, 129.2, 126.9, 125.4, 102.0, 100.4, 99.0, 98.1, 89.3, 85.9, 60.5, 56.4, 31.4, 30.6, 30.4, 29.8, 27.2, 18.6, 18.5, 18.0, 17.9, 9.4, 8.9, 8.8, 8.7, 8.7. UV-vis (CH₂Cl₂) λ_{max} (log ε): 379 (4.64), 402 (4.68), 513 (3.69), 549 (3.91), 594 (3.85), 648 (4.01); fluorescence (CH₂Cl₂, $\lambda_{\text{excitation}} = 402$ nm) $\lambda_{\text{max-emission}} = 689$ nm. IR (diamond ATR, neat): 1675 (v_{C=O}), 3458, 3366 (v_{N-H}) cm⁻¹. As with other osmate esters,²¹ we could not acquire a [M]⁺ or [M-H]⁻ mass spectrum of this species albeit we observed [M]⁺ for the corresponding dihydroxy species **11-O^{7,17}(OH)^{2,3}**: HR-MS (ESI+, 100% CH₃CN, TOF): calc'd for C₃₆H₄₈N₄O₃ [M]⁺ 600.3676, found 600.3578.

followed by 10% acetone in CH₂Cl₂. MW = 977.204 g/mol; R_f = 0.29 (silica- 10% acetone in CH₂Cl₂). ¹H NMR (400 MHz, CDCl₃): δ 8.86 (d, ³J_{H,H} = 8.7 Hz, 2H), 8.69 (d, ³J_{H,H} = 10.9 Hz, 2H), 8.43 (s, 1H), 7.88 (s, 1H), 7.74 (s, 1H), 7.65 (d, ³J_{H,H} = 4.5 Hz, 2H), 7.48 (d, ³J_{H,H} = 9.0 Hz, 2H), 7.35 (s, 2H), 7.05 (s, 1H), 3.61 (s, 1H), 3.41 – 3.31 (m, 4H), 3.20 (s, 1H), 2.95 – 2.81 (m, 2H), 2.71 – 2.61 (m, 2H), 2.31 – 2.15 (m, 8H), 1.53 – 1.46 (m, 9H), 0.92 (t, ³J_{H,H} = 7.4 Hz, 3H), 0.58 – 0.42 (m, 12H). ¹³C{¹H} NMR (101 MHz, CDCl₃): δ 209.7 (C=O), 209.4 (C=O), 169.6, 155.4, 154.6, 152.4, 152.2, 150.8, 149.7, 142.8, 142.1, 135.1, 131.9, 129.2, 126.9, 125.4, 102.0, 100.4, 99.0, 98.1, 89.3, 85.9, 60.5, 56.4, 31.4, 30.6, 30.4, 29.8, 27.2, 18.6, 18.5, 18.0, 17.9, 9.4, 8.9, 8.8, 8.7, 8.7. UV-vis (CH₂Cl₂) λ_{max} (log ε): 379 (4.64), 402 (4.68), 513 (3.69), 549 (3.91), 594 (3.85), 648 (4.01); fluorescence (CH₂Cl₂, $\lambda_{\text{excitation}} = 402$ nm) $\lambda_{\text{max-emission}} = 689$ nm. IR (diamond ATR, neat): 1675 (v_{C=O}), 3458, 3366 (v_{N-H}) cm⁻¹. As with other osmate esters,²¹ we could not acquire a [M]⁺ or [M-H]⁻ mass spectrum of this species albeit we observed [M]⁺ for the corresponding dihydroxy species **11-O^{7,17}(OH)^{2,3}**: HR-MS (ESI+, 100% CH₃CN, TOF): calc'd for C₃₆H₄₈N₄O₃ [M]⁺ 600.3676, found 600.3578.

ASSOCIATED CONTENT

Supporting Information

Reproduction of the UV-vis, fluorescence, ¹H, ¹³C, and mass spectra of all novel compounds. FAIR Data is available as Supporting Information for Publication and includes the primary NMR FID files for compounds: **8-O^{2,7,12}** and **8-O^{2,7,18}** (included for comparison), **9-O^{2,12}(OH)^{7-rac}, **9-O^{7,18}(OH)^{2-rac}, **10-O²(OH)^{7,12-syn}, **10-O²(OH)^{7,12-anti}**, **11-O^{7,17}(O-**osmate**)^{2,3-rac}, **12-O^{3,7}(OH)^{7,18-rac}, and **13-O^{2,7}(OH)^{17,18-rac}**.** See [FID for Publication](#) for additional information. Experimental details for the crystal structure determinations of **9-O^{2,12}(OH)^{7-rac}** (CCDC # 2149409) and **10-O²(OH)^{7,12-anti}** (CCDC # 2149408) (PDF), including the .cif files. The .cif files can also be obtained free of charge from The Cambridge Crystallographic Data Centre via [www.ccdc.cam.ac.uk/data_request/cif](#). The Supporting Information is available free of charge on the ACS Publications website.********

AUTHOR INFORMATION

Corresponding Author

* nivedita.chaudhri@uconn.edu (NC) and c.bruckner@uconn.edu (CB)

Present Addresses

† Department of Molecular Biophysics and Biochemistry, Yale University, New Haven, CT, U.S.A.; Microbial Sciences Institute, Yale University, West Haven, CT, U.S.A.

Author Contributions

NC devised and executed majority of the study and wrote the first draft manuscript. MGF performed all computations. MZ performed all single crystal diffractometry analyses. CB oversaw the study and wrote the final manuscript with input from all authors. All authors have given approval to the final version of the manuscript.

ACKNOWLEDGMENT

This work was supported by the US National Science Foundation under Grant Number CHE-1800361 (to CB). The X-ray diffractometer was funded by NSF Grant CHE-1625543 (to MZ). We thank Chi-Kwong (Chris) Chang, Michigan State University, for a donation of OEP used in this study.

REFERENCES

- (1) (a) Montforts, F.-P.; Gerlach, B.; Höper, F. Discovery and Synthesis of Less Common Natural Hydroporphyrins. *Chem. Rev.* **1994**, *94*, 327–347; (b) Brückner, C.; Samankumara, L.; Ogikubo, J. In *Handbook of Porphyrin Science*; Kadish, K. M., Smith, K. M., Guilard, R., Eds.; World Scientific: Singapore, 2012; Vol. 17, p 1–112; (c)

Taniguchi, M.; Lindsey, J. S. Synthetic Chlorins, Possible Surrogates for Chlorophylls, Prepared by Derivatization of Porphyrins. *Chem. Rev.* **2017**, *117*, 344–353.

(2) Gouterman, M. In *The Porphyrins*; Dolphin, D., Ed.; Academic Press: New York, 1978; Vol. 3, p 1–165.

(3) (a) Johansen, J. E.; Piermattei, V.; Angst, C.; Diener, E.; Kratky, C.; Eschenmoser, A. Interconversion of the Chromophore Systems of Porphyrinogen and 2,3,7,8,12,13-Hexahydroporphyrin. *Angew. Chem., Int. Ed. Engl.* **1981**, *20*, 261–263; (b) Lahiri, G. K.; Stolzenberg, A. M. Reductive Chemistry of Nickel Hydroporphyrins. 3. Facile Preparation of Hexahydroporphyrin Complexes by Reduction of (Octaethylisobacteriochlorin)Nickel(II). *Angew. Chem., Int. Ed. Engl.* **1993**, *32*, 429–432; (c) Lash, T. D.; Hall, T.; Mani, U. N.; Jones, M. A. Normal and Abnormal Heme Biosynthesis. 3.1 Synthesis and Metabolism of Tripromionate Analogues of Coproporphyrinogen-III: Novel Probes for the Active Site of Coproporphyrinogen Oxidase. *J. Org. Chem.* **2001**, *66*, 3753–3759.

(4) (a) Waditschatka, R.; Kratky, C.; Jaun, B.; Heinzer, J.; Eschenmoser, A. Chemistry of Pyrrocorphins: Structure of Nickel(II) ccccc-Octaethylpyrrocophilane in the Solid State and in Solution. Observation of the Inversion Barrier between Enantiomorphically Ruffled Conformers. *J. Chem. Soc., Chem. Commun.* **1985**, 1604–1607; (b) Waditschatka, R.; Eschenmoser, A. Chemistry of Pyrrocorphins: Stereoselectivity During Porphyrinogen - Pyrrocophilane Tautomerism. *Angew. Chem.* **1983**, *95*, 639–640; (c) Waditschatka, R.; Diener, E.; Eschenmoser, A. Chemistry of Pyrrocorphins: Carbon Methylation of Pyrrocophilanes on the Ligand Periphery. *Angew. Chem.* **1983**, *95*, 641–642; (d) Eschenmoser, A. Chemistry of Corphins. *Ann. NY Acad. Sci.* **1986**, *471*, 108–129; (e) Summers, J. S.; Stolzenberg, A. M. The *cis*-Influence of Hydroporphyrin Macrocycles on the Axial Ligation Equilibria of Co(II) and Zn(II) Porphyrin Complexes. *J. Am. Chem. Soc.* **1993**, *115*, 10559–10567.

(5) (a) Smith, K. M.; Simpson, D. J. Raney Nickel Reductions of Chlorophyll Derivatives: Hydroporphyrin in the Anhydro Series. *J. Am. Chem. Soc.* **1987**, *109*, 6326–6333; (b) De Voss, J. J.; Leeper, F. J.; Battersby, A. R. Synthetic Studies Relevant to Biosynthetic Research on Vitamin B₁₂. Part 12. Modification of the Periphery of Chlorins and Isobacteriochlorins. *J. Chem. Soc., Perkin Trans. I* **1997**, 1105–1116.

(6) (a) Ide, Y.; Kuwahara, T.; Takeshita, S.; Fujishiro, R.; Suzuki, M.; Mori, S.; Shinokubo, H.; Nakamura, M.; Yoshino, K.; Ikeue, T. Nickel (II) Pyrrocophilane: Enhanced Binding Ability in a Highly Reduced Porphyrin Complex. *J. Inorg. Biochem.* **2018**, *178*, 115–124; (b) Silva, A. M. G.; Tomé, A. C.; Neves, M. G. P. M. S.; Silva, A. M. S.; Cavaleiro, J. A. S. 1,3-Dipolar Cycloaddition Reactions of Porphyrins with Azomethine Ylides. *J. Org. Chem.* **2005**, *70*, 2306–2314; (c) Yu, Y.; Furuyama, T.; Tang, J.; Wu, Z.-Y.; Chen, J.-Z.; Kobayashi, N.; Zhang, J.-L. Stable Iso-Bacteriochlorin Mimics from Porpholactone: Effect of a β -Oxazolone Moiety on the Frontier π -Molecular Orbitals. *Inorg. Chem. Front.* **2015**, *2*, 671–677; (d) Peters, M. K.; Röhricht, F.; Näther, C.; Herges, R. One-Pot Approach to Chlorins, Isobacteriochlorins, Bacteriochlorins, and Pyrrocorphins. *Org. Lett.* **2018**, *20*, 7879–7883.

(7) Fischer, H.; Orth, H. *Die Chemie Des Pyrrols*; Akademische Verlagsgesellschaft (Johnson Reprint, New York 1968); Leipzig, 1937; Vol. II, Part I.

(8) (a) Bonnett, R.; Dolphin, D.; Johnson, A. W.; Oldfield, D.; Stephenson, G. F. Oxidation of Porphyrins with H₂O₂ in H₂SO₄. *Proc. Chem. Soc.* **1964**, 371–372; (b) Bonnett, R.; Dimsdale, M. J.; Stephenson, G. F. *meso*-Reactivity of Porphyrins and Related Compounds. IV. Introduction of Oxygen Functions. *J. Chem. Soc. C* **1969**, 564–570.

(9) (a) Inhoffen, H. H.; Nolte, W. Chlorophyll and Hemin. XXIV. Oxidative Rearrangements of Octaethylporphine to Geminiporphine Polyketones. *Justus Liebigs Ann. Chem.* **1969**, *725*, 167–176; (b) Chang, C. K. Synthesis and Characterization of Alkylated Isobacteriochlorins, Models of Siroheme and Sirohydrochlorin. *Biochemistry* **1980**, *19*, 1971–1976; (c) Brückner, C.; Chaudhri, N.; Nevonen, D. E.; Bhattacharya, S.; Graf, A.; Kaesemann, E.; Li, R.; Guberman-Pfeffer, M. J.; Mani, T.; Nimthong-Roldán, A.; Zeller, M.; Chauvet, A. A. P.; Nemykin, V. Structural and Photophysical Characterization of All Five Constitutional Isomers of the Octaethyl-

β,β' -Dioxo-Bacterio- and -Isobacteriochlorin Series. *Chem.—Eur. J.* **2021**, *27*, 16189–16203.

(10) Chaudhri, N.; Guberman-Pfeffer, M. J.; Li, R.; Zeller, M.; Brückner, C. β -Trioxopyrrocorphins: Pyrrocorphins of Graded Aromaticity. *Chem. Sci.* **2021**, *12*, 12292–12301.

(11) (a) Kadish, K. M.; E. W.; Zhan, R.; Khouri, T.; Goenlock, L. J.; Prashar, J. K.; Sintic, P. J.; Ohkubo, K.; Fukuzumi, S.; Crossley, M. J. Porphyrin-Diones and Porphyrin-Tetraones: Reversible Redox Units Being Localized within the Porphyrin Macrocycle and Their Effect on Tautomerism. *J. Am. Chem. Soc.* **2007**, *129*, 6576–6588; (b) Ke, X.-S.; Chang, Y.; Chen, J.-Z.; Tian, J.; Mack, J.; Cheng, X.; Shen, Z.; Zhang, J.-L. Porphidilactones as Synthetic Chlorophylls: Relative Orientation of β -Substituents on a Pyrrolic Ring Tunes NIR Absorption. *J. Am. Chem. Soc.* **2014**, *136*, 9598–9607; (c) Brückner, C.; Ogikubo, J.; McCarthy, J. R.; Akhigbe, J.; Hyland, M. A.; Daddario, P.; Worlinsky, J. L.; Zeller, M.; Engle, J. T.; Ziegler, C. J.; Ramaghan, M. J.; Sandberg, M. N.; Birge, R. R. Oxazolochlorins. 6. *meso*-Arylporpholactones and Their Reduction Products. *J. Org. Chem.* **2012**, *77*, 6480–6494; (d) Guberman-Pfeffer, M. J.; Lalisse, R. F.; Hewage, N.; Brückner, C.; Gascón, J. A. Origins of the Electronic Modulations of Bacterio- and Isobacteriolactone Regiosomers. *J. Phys. Chem. A* **2019**, *123*, 7470–7485.

(12) Yao, Y.; Rao, Y.; Liu, Y.; Jiang, L.; Xiong, J.; Fan, Y. J.; Shen, Z.; Sessler, J. L.; Zhang, J. L. Aromaticity Versus Regiosomeric Effect of β -Substituents on Porphyrinoids. *Phys. Chem. Chem. Phys.* **2019**, *21*, 10152–10162.

(13) (a) Adams, K. R.; Berenbaum, M. C.; Bonnett, R.; Nizhnik, A. N.; Salgado, A.; Valles, M. A. Second Generation Tumour Photosensitisers: The Synthesis and Biological Activity of Octaalkyl Chlorins and Bacteriochlorins with Graded Amphiphilic Character. *J. Chem. Soc., Perkin Trans. I* **1992**, 1465–1470; (b) Li, R.; Zeller, M.; Bruhn, T.; Brückner, C. Surprising Outcomes of Classic Ring-Expansion Conditions Applied to Octaethylloxochlorin, 3. Schmidt-Reaction Conditions. *Eur. J. Org. Chem.* **2017**, 1835–1842 and references therein; (c) Cai, S.; Belikova, E.; Yatsunyk, L. A.; Stolzenberg, A. M.; Walker, F. A. Magnetic Resonance and Structural Investigations of (Monooxoctaethylchlorinato)Iron(III) Chloride and Its Bis(Imidazole) Complex. *Inorg. Chem.* **2005**, *44*, 1882–1889; (d) Papkovsky, D. B.; Ponamorev, G. V.; Trettnak, W.; O’Leary, P. Phosphorescent Complexes of Porphyrin Ketones: Optical Properties and Application to Oxygen Sensing. *Anal. Chem.* **1995**, *67*, 4112–4117; (e) Barkigia, K. M.; Chang, C. K.; Fajer, J.; Renner, M. W. Models of Heme D1. Molecular Structure and NMR Characterization of an Iron(III) Dioxoisobacteriochlorin (Porphyrindione). *J. Am. Chem. Soc.* **1992**, *114*, 1701–1707; (f) Schnable, D.; Chaudhri, N.; Li, R.; Zeller, M.; Brückner, C. Evaluation of Octaethyl-7,17-Dioxobacteriochlorin as a Ligand for Transition Metals. *Inorg. Chem.* **2020**, *59*, 2870–2880 and references therein; (g) Fujii, H.; Yamaki, D.; Ogurac, T.; Hadab, M. The Functional Role of the Structure of the Dioxoisobacteriochlorin in the Catalytic Site of Cytochrome c₁ for the Reduction of Nitrite. *Chem. Sci.* **2016**, *7*, 2896–2906; (h) Taniguchi, M.; Kim, H.-J.; Ra, D.; Schwartz, J. K.; Kirmaier, C.; Hindin, E.; Diers, J. R.; Prathapan, S.; Bocian, D. F.; Holten, D.; Lindsey, J. S. Synthesis and Electronic Properties of RegiosomERICALLY Pure Oxochlorins. *J. Org. Chem.* **2002**, *67*, 7329–7342.

(14) (a) Connick, P. A.; Macor, K. A. Spectroscopic and Electrochemical Characterization of Nickel β -Oxoporphyrins: Identification of Nickel(III) Oxidation Products. *Inorg. Chem.* **1991**, *30*, 4654–4663; (b) Connick, P. A.; Haller, K. J.; Macor, K. A. X-Ray Structural and Imidazole-Binding Studies of Nickel β -Oxoporphyrins. *Inorg. Chem.* **1993**, *32*, 3256–3264; (c) Connick, P. A. Electrochemical Titrations of Nickel β -Oxoporphyrins with Imidazole. *Electrochem. Soc. Interface* **1993**, *2*, 51–52; (d) Turowska-Tyrk, I.; Kang, S.-J.; Scheidt, W. R. Conformational Distortions of π -Cation Radical (β -Oxoporphyrin)Copper(II) Derivatives: [Cu(2,7,12-TrioxoOEHP)][SbCl₆] and [Cu(2,7-DioxoOEBC)][SbCl₆]. *J. Porphyrins Phthalocyanines* **2011**, *15*, 373–381; (e) Nganga, J.; Chaudhri, N.; Brückner, C.; Angeles-Boza, A. M. β -Oxochlorin Cobalt(II) Complexes Catalyze the Electrochemical Reduction of CO₂. *Chem. Commun.* **2021**, *57*, 4396–4399.

(15) (a) Chaudhri, N.; Zeller, M.; Brückner, C. Stepwise Reduction of Octaethyl- β,β' -Dioxochlorin Isomers: Access to Structurally and Electronically Diverse Hydroporphyrins. *J. Org. Chem.* **2020**, *85*, 13951–13964; (b) Nguyen, K.-U.; Zhang, R.; Taniguchi, M.; Lindsey, J. S. Fluorescence Assay for Tolyporphins Amidst Abundant Chlorophyll in Crude Cyanobacterial Extracts. *Photochem. Photobiol.* **2021**, *97*, 1507–1515.

(16) (a) Mass, O.; Ptaszek, M.; Taniguchi, M.; Diers, J. R.; Kee, H. L.; Bocian, D. F.; Holten, D.; Lindsey, J. S. Synthesis and Photochemical Properties of 12-Substituted versus 13-Substituted Chlorins. *J. Org. Chem.* **2009**, *74*, 5276–5289; (b) Liu, M.; Chen, C.-Y.; Hood, D.; Taniguchi, M.; Diers, J. R.; Bocian, D. F.; Holten, D.; Lindsey, J. S. Synthesis, Photophysics and Electronic Structure of Oxobacteriochlorins. *New J. Chem.* **2017**, *41*, 3732–3744.

(17) Falk, H. *The Chemistry of Linear Oligopyrroles and Bile Pigments*; Springer Verlag: Wien, New York, 1989.

(18) Jentzen, W.; Song, X.-Z.; Shelnutt, J. A. Structural Characterization of Synthetic and Protein-Bound Porphyrins in Terms of the Lowest-Frequency Normal Coordinates of the Macrocycle. *J. Phys. Chem. B* **1997**, *101*, 1684–1699.

(19) (a) Kingsbury, C. J.; Senge, M. O., The shape of porphyrins. *Coord. Chem. Rev.* **2021**, *431*, 213760. (b) <https://kingsbury.pythongithub.io/nsd>, accessed 6/2020

(20) Kratky, C.; Waditschatka, R.; Angst, C.; Johansen, J. E.; Plaquevent, J. C.; Schreiber, J.; Eschenmoser, A. Die Sattelkonformation Der Hydrophorphinoiden Ni(II)-Komplexe: Struktur, Ursprung, und Stereochemische Konsequenzen. *Helv. Chim. Acta* **1985**, *68*, 1312–1337.

(21) Hewage, N.; Daddario, P.; Lau, K. S. F.; Guberman-Pfeffer, M. J.; Gascón, J. A.; Zeller, M.; Lee, C. O.; Khalil, G. E.; Gouterman, M.; Brückner, C. Bacterio- and Isobacteriodilactones by Stepwise or Direct Oxidations of *meso*-Tetrakis(pentafluorophenyl)porphyrin. *J. Org. Chem.* **2019**, *84*, 239–256.

(22) Samankumara, L. P.; Zeller, M.; Krause, J. A.; Brückner, C. Syntheses, Structures, Modification, and Optical Properties of *meso*-Tetraaryl-2,3-Dimethoxychlorin, and Two Isomeric *meso*-Tetraaryl-2,3,12,13-Tetrahydroxybacteriochlorins. *Org. Biomol. Chem.* **2010**, *8*, 1951–1965.

(23) (a) Schwesinger, R.; Waditschatka, R.; Rigby, J.; Nordmann, R.; Schweizer, W. B.; Zass, E.; Eschenmoser, A. Das Pyrrocophin-Ligandsystem: Synthese des 2,2,7,7,12,12,17-Heptamethyl-2,3,7,8,12,13-Hexahydroporphyrins. *Helv. Chim. Acta* **1982**, *65*, 600–610; (b) Abraham, R. J.; Medforth, C. J.; Smith, K. M.; Goff, D. A.; Simpson, D. J. NMR Spectra of Porphyrins. Part 31. Ring Currents in Hydroporphyrins. *J. Am. Chem. Soc.* **1987**, *109*, 4786–4791.

(24) (a) Becke, A. D. Density-Functional Thermochemistry. III. The Role of Exact Exchange. *J. Chem. Phys.* **1993**, *98*, 5648–5652; (b) Weigend, F.; Ahlrichs, R. Balanced Basis Sets of Split Valence, Triple Zeta Valence and Quadruple Zeta Valence Quality for H to Rn: Design and Assessment of Accuracy. *Phys. Chem. Chem. Phys.* **2005**, *7*, 3297–3305.

(25) Ogikubo, J.; Meehan, E.; Engle, J. T.; Ziegler, C. J.; Brückner, C. Oxazolochlorins. 9. *meso*-Tetraphenyl-2-Oxabacteriochlorins and *meso*-Tetraphenyl-2,12/13-Dioxabacteriochlorins. *J. Org. Chem.* **2013**, *78*, 2840–2852 and references therein.

(26) Fliegl, H.; Valiev, R. R.; Pichierri, F.; Sundholm, D. M. B., Theoretical studies as a tool for understanding the aromatic character of porphyrinoid compounds. *Chem. Modell.* **2018**, *14*, 1–42.

Insert Table of Contents artwork here

